WIS-87/68/Sept-PH

A HIGHLY EFFICIENT LOW-PRESSURE UV-RICH DETECTOR WITH OPTICAL AVALANCHE RECORDING

A. Breskin, R. Chechik,* Z. Fraenkel, D. Sauvage, V. Steiner and I. Tserruya
Weizmann Institute, Rehovot, Israel

G. Charpak, W. Dominik, J.P. Fabre, J. Gaudean, F. Sauli and M. Suzuki
CERN, Geneva, Switzerland

P. Fischer, P. Glässel, H. Ries, A. Schön and H. Specht
University of Heidelberg, Heidelberg, Germany

Abstract

UV photons from a Čerenkov radiator are multiplied in a multistep avalanche chamber operating in a gated mode at low gas pressure (40 Torr). The gas mixture is C_2H_6 –argon(80/20) and TMAE at 34°C. Visible light emitted from single photoelectron avalanches is detected by a CCD camera coupled to an image intensifier system. The detector was tested with 5 GeV/c electrons using a CH_4 radiator gas at 1 atmosphere. Čerenkov rings esse[redacted]dary photon feed-back were obtained in this m[redacted] : n≅10 (N_o ≅68 cm^{-1}). We present this new me[redacted]

Presented at the London Conference on Position Sensitive Detectors
London, 7-11 September, 1987

(To be published in Nucl. Instrum. Methods)

* The Hettie H. Heineman Research Fellow

1. Introduction

A multistep avalanche chamber, operating at low gas pressure (LPMSC) with a photosensitive mixture is an efficient tool for the imaging of single UV-photons[1,2]. A LPMSC was proposed as a UV-photon detector for Čerenkov ring imaging (RICH), in relativistic heavy ion experiments (HELIOS-CERN)[3], and it was recently shown that a detector of this type can be applied for recording multiple photon events[4]. In this kind of experiments the detector has to record several simultaneous Čerenkov rings per event (~10 rings/event in S + Au at 200 GeV/u), in the presence of a high background consisting of high energy photons and charged particles. The main advantages in using LPMSC's are [1,2]: high gain ($10^7 - 10^8$), reduced photon feedback, low sensitivity to background radiation (low dE/dx), low self-absorption of UV-photons in the carrier gas, high rate capability and the possibility of gating the detector on events of interest.

The position sensing with wire chambers is usually done using wire readout electronics, recording the avalanche induced charges on several wire planes. However, when many simultaneous particles, complex particle events or multiple Čerenkov rings are to be recorded, the readout electronics becomes very sophisticated and expensive. In order to achieve maximum redundancy, parameters like pulse height and time have to be recorded in addition to the position coordinates, using multihit electronics like flash ADC's, as in the case of drift chambers[5] or multistep chambers[3]. A genuine two-dimensional pad-structured readout is thus the natural solution and some efforts have been made in this direction, for example in endcup detectors for TPC's[6]. Some devel-

A considerable step forward was made by realizing that replacing TEA by TMAE [tetrakis(dimethylamine)ethylene], which emits in the visible (peaked at 480 nm)[17], provides a light/charge yield comparable to that of TEA, for equal vapor concentrations and operation pressures[15].

The emission in the visible range is of great advantage since standard, high aperture lenses and standard image intensifiers can be used. Moreover, TMAE has the largest quantum efficiency[18], among known photosensitive vapors, in the UV range (120-230 nm).

A systematic study of light emission from Argon-TMAE and C_2H_6 or CH_4 mixtures was carried on and it was found that a light/charge ratio of the order of 0.1 can be reached at low gas pressures in mixtures having gain and diffusion properties suitable for the application to RICH[15]. Using LPMSC's, 10^6-10^7 secondary visible photons can be emitted per single photoelectron avalanche which is sufficient to make the detection of single photoelectrons possible and efficient.

We have built a prototype of a 3-stage gated UV-photon detector[19] and have studied the application to RICH with a 5 GeV/c electron beam at the CERN-PS. In the present setup, we recorded on the average $\bar{n} \cong 10$ photoelectrons per Čerenkov ring, which corresponds to an N_0 value of 70 cm^{-1}. The localization resolution per single photon is $\sigma \cong 2.2$ mm, mostly due to chromatic aberration and diffusion. We describe here the detector, its optical system and the experimental setup, and present preliminary results.

opment is presently being done in applying pad readout in MWPC's or LPMSC's for RICH[7].

Another 2D localization method is the optical recording of electron avalanches. The idea of recording the light produced by inelastic collisions during the avalanche process was put forward a few years ago[8-12]. It was clear that using a "photographic" technique would have many advantages for recording complex events, but the small amount of light usually produced in the avalanche, and its unfavorable spectral properties (in most cases the emission is in the far UV-range), made this detection a non-trivial task. The possibility of shifting the UV-radiation into the visible was proposed, using an appropriate organic fluor coating of the detector anode[10]. Another way was to search for an efficient gas mixture which could yield a large amount of light at convenient wavelengths. In the last few years an active research was carried out in this domain and it was found that high light yields can be reached by mixing TEA (triethylamine) vapours with Ar, Kr and Xe and hydrocarbons[13]. This is due to an efficient process of resonant energy transfer from the noble gas atoms to the TEA molecules. A light yield of 1-4 secondary photons was measureed, at normal gas pressure, per single secondary electron produced in the detector volume[14,15]. Successful attempts were made to image particle tracks using MWPC's[16] and parallel grid chambers[14] operating at normal gas pressures with Ar/CH_4/TEA-80/18/2. The TEA emission being in the UV (peaked at 280 nm)[13], UV optics and a UV sensitive image intensifier had to be used, coupled to a Vidicon camera and finally to a CCD device.

any further charge amplification.

3. The optical read-out

3.1 Light emission from TMAE mixtures

Fig. 2 shows the light emission spectrum as recorded using a parallel grid chamber coupled to a monochromator. The gas, Argon (98), CH_4(2), TMAE (23°C), at atmospheric pressure, was excited by α-particles from a ^{241}Am source. The spectrum, peaked at about 480 nm, is in agreement with data obtained from TMAE excitation by UV photons (250-390 nm)[17]. An example of the light/charge yield in a gas mixture used in the present work, namely C_2H_6 (80) Argon (20) TMAE, is shown in fig. 3. The light yield was measured as a function of pressure and TMAE concentration by recording charge and light emitted from electron avalanches, initiated by 5.9 keV x-rays from a ^{55}Fe source, in a parallel grid chamber. A detailed description is given elsewhere[15]. It was found that the light yield is indeed a function of the TMAE partial pressure (temperature).

3.2 The optical readout system

The optical recording system is shown in fig. 4. It is composed of the following elements:

1. Large aperture lens, Leitz Noctilux 1:1/50 mm.
2. A gateable MCP image intensifier, Philips XX1410
   - active diameter: 18mm

2. The UV detector

The UV photon detector is a multistep avalanche chamber operated in a gated mode[20], at a low gas pressure, of 40 Torr of C_2H_6/Ar (80/20)+TMAE at 34°C. The detector is schematically shown in Fig. 1. It has an active area of 20×20 cm^2 and is built in a modular structure of epoxy resin – and delrin frames intersealed with Viton o-rings. All the electrodes are made of stainless steel mesh with 81% transparency. Incident UV photons are converted to electrons in the conversion region; its width of 30 mm corresponds to L=3λ, λ being the photon absorption length of TMAE at 34°C[2]. The electrons drift to a first amplification stage, operated in a parallel plate avalanche mode. A fraction of the preamplified electron swarm drifts towards the gate device, formed by two meshes having between them a normally reversed field. The charges can be transmitted further towards the second amplification stage if the electric field is set to a correct value and direction, by applying a negative pulse on electrode 4 (see fig. 1). The gate pulse has to be applied at a proper time after the formation of the preamplified avalanche. It has to have a width larger or equal to the drift time of the electrons in the conversion region, so as to ensure full efficiency of the photon detection. The second amplification stage is also made of two grids, operating in a parallel-plate avalanche mode. Electrons are further transferred to a third parallel mesh element. The electric field in this stage is high but below charge amplification threshold. Electrons drifting across the gap of this element produce light by excitation of the gas molecules. This last stage is indeed responsible for an increase of the light emission by at least an order of magnitude, without

photon (at 480 nm) at the photocathode. The light gain of the reducing intensifier is 7, this giving a total light gain of $1.4 \cdot 10^4$. The demagnification factor in the present experiment is of the order of 12.

4. Experimental set-up for RICH

The UV detector described in section 2 is coupled via a UV-transparent window to a gas radiator. The window is made of four slabs of 10×10 cm^2 7 mm thick each, two of them are made of CaF_2 and two are Suprasil quartz. The radiator set-up is identical to that described in ref. 3), except for a longer focal length of 1.7m of the spherical UV mirror mounted inside the radiator tank. The radiator operates in a flow mode with CH_4 gas at 1 atmosphere, using a 99.95% pure gas and an "oxisorb" filter. The tank is pumped to below 10^{-5} Torr before the filling. The UV transmission of the radiator gas is continuously monitored in the wavelength range of 150-220 nm. The monitor consists of a UV-monochromator coupled to a 1 m long stainless steel tube, with the radiator gas continuously flowing through it. With the present system we have measured a transmission of about 0.9 in the range of 160-220 nm.

The UV detector is operated in a flow mode with 40 Torr of C_2H_6/Ar-80/20 (both 99.995% pure + oxysorb), bubbling through a liquid TMAE bubbler, which is immersed in a bath at 34°C. At this temperature the percentage of TMAE vapors is of 2.4%. The gas flow system of the detector is described in more detail in ref. 2). The detector and all the gas tubings are heated to about 40°C, to prevent TMAE condensation on walls

- photocathode: S20
- phosphor: P36, decay-time 250 ns

3. Image intensifier and reducer, DEP XX1490
   - active diameter: ϕ_{in}=18mm to ϕ_{out}=7mm
   - photocathode: S20
   - phosphor: P46, decay-time 100 ns
4. CCD camera, Thomson TH 7852 FO
   - active area: 4.32×5.82 mm^2
   - pixels: 144×208
5. Video digitizer: Data Translation DT 2851
6. Computer: IBM PC/AT

The two image intensifiers and the CCD camera are coupled to each other via optical fibers. The first image intensifier can operate either in a continuous mode or in a gated mode. In the latter case, the potential between the photocathode and the MCP cathode is reversed and is set to a proper value only upon the application of a HV pulse of 280 V, triggered by a main trigger system as for the detector gate. The gating of the MCP intensifier and the use of fast phosphors considerably reduces the "noise" from light penetration and "old" events. The video digitizer runs synchronously at 25 Hz. When a trigger occurs, the corresponding frame is stored.

Taking into account the quantum efficiencies of the photocathodes and the phosphor efficiencies, the light gain of the first intensifier is $2 \cdot 10^3$ secondary photons per single

detector nor the MCP image intensifier were operated at their maximum gain. Though normally the lens was used with an aperture of F=1, we could observe the photons without substantial losses up to F=4.

5. Results

Examples of typical Čerenkov rings (4 consecutive events) are shown in fig. 5. One can sees that due to the low pressure operation and the gating of both the detector and the image intensifier the rings are free from background and of photon feedback avalanches. Fig. 6 shows the light distribution from single photon avalanches obtained from a sample of 95 events. It has an exponential behaviour, typical of single electron avalanches at a relatively low gain, non-saturated operation mode. We have measured the absolute number of photons per avalanche, by using a calibrated green LED and replacing the optical chain, that follows the lens, by a photomultiplier. We measured a mean value of about 1000 visible photons per avalanche, at the present solid angle (demagnification factor 12), as shown in fig. 6. Taking into account the light gain of the image intensifiers we get on the average more than 10^7 photons on the CCD, per initial UV photon! The light spots are rather broad, due to a considerable size of the avalanche in the LPMSC, and spread over about 100 pixels, which makes the calculation of the centroid a rather simple task. The average signal-to-noise per pixel is of the order of 100. The size of the light spots may be reduced by reducing the length of the transfer gap in the UV detector and correspondingly increasing the TMAE temperature and the

and windows of the detector. The gas is pumped out through a cold trap at -30°C, to prevent TMAE vapours from contaminating the pump.

The RICH prototype was tested with a beam of 5 GeV/c electrons from the PS accelerator at CERN. A pair of threshold Čerenkov counters and appropriate scintillators provided the beam trigger for the detector and image intensifier gates and for the computer digitizing system. A negative gating pulse of 40 V was applied to electrode 4 (see fig. 1) at the proper time. The gate pulse duration was about 2 μs, to allow the full transmission of the preamplified electron avalanche.

The gating of the UV detector proved to be essential in this experiment. It made the detector blind to most of the background radiation, enabling an operation at high gains. Furthermore, it prevented the second amplification stage from detecting delayed parasitic secondary avalanches, due to photon feedback.

Within the gate period the UV detector had a gain of about 10^7; the operating voltages were: HV1=0, HV2=100V, HV3=980V, HV4=1320V, HV5=1300V, HV6=1600V, HV7=2320V, HV8=2890V.

The optical readout system was coupled to the rear end of the UV detector through a ϕ 180mm quartz window, mounted at about 30mm from the last electrode (No. 8). The image intensifier was operated in a pulsed mode, with a pulse generated from the beam trigger, with a duration varied from 10–500 μs.

With the present video digitizing system used for this test run, several rings could be detected per beam burst (480 ms). Due to the high photon yield, neither the UV-

reach on the average about 1000 photons per single UV photon, on the photocathode of the first image intensifier – which makes the system practically free of noise.

The N_o value of the UV-detector was calculated using the data of fig. 9. The window was made of CaF_2/Suprasil (50/50). Taking into consideration the cutoff of C_2H_6, quantum efficiency of TMAE and the transmission of Suprasil, we get a theoretical value of $< N_o >_{th}$=158 cm^{-1}. However, the efficiency of the radiator and the detector system is affected by several losses:

- mirror reflectivity: 0.85
- transmission of the radiator gas: 0.90
- transmission of the window frame: 0.94
- losses due to a 1 mm distance between the window and the first mesh: 0.90
- transmission of the first mesh: 0.81
- efficiency of the 3λ conversion gap: 0.95

The total efficiency is therefore only of 0.5, yielding an expected value of $< N_o >$=79 cm^{-1}.

Taking into account the radiator length of 1.41 m and a $\gamma_{TH} \cong 30.6$, the expected number of photoelectrons should be $(\bar{n})$=11.9. We have measured experimentally an average number of 10.2 photons corresponding to $N_o \cong 68$ cm^{-1}. This is in reasonable agreement with the calculated value regarding the preliminary stage of the data analysis. With an improved design of the detector, an efficiency of at least 0.7 should be obtainable.

gas pressure.

Rings with fixed radius (R=52 mm) were fitted to the data. The radial distribution of the centers of gravity of the light spots is shown on fig. 7. The distribution has an rms width of 2.2 mm, very similar to that obtained using a FADC electronic readout[3]. The major contributions to this width come from the diffusion of single electrons in the conversion gap ($\sigma \cong 1.1$ mm) and from chromatic aberrations ($\sigma \cong 1.3$ mm). The contribution of the readout system is negligible due to the excellent signal-to-noise ratio.

The distribution of the number of photoelectrons is shown in fig. 8. The mean value is 10.2 photons. The minimum number of photons is 6. The "zero" events correspond to sparks in the detector – due to a bad isolation between the metal frame of the window and the last electrode, and to empty frames – due to some inefficiency of the computer trigger. It should be noted that the distribution of the number of photons is based on a preliminary on-line analysis of 95 events. The photon finding algorithm was not optimized and spatial pile-up losses were not corrected for.

6. Discussion and conclusions

We have shown that a combination of a low-pressure multistep UV-photon detector and an optical readout may be an efficient solution for recording Čerenkov rings. The optical readout provides a real, unambiguous, 2D localization of single photons, which is crucial for recording multiple Čerenkov rings.

The considerable light yield of TMAE and the high detector gain enables us to

We would like to thank Mrs. J. Gil, Mr. J. Asher, Mr. G. Lamade and Mr. M. Klin for technical assistance. We are indebted to Mr. R. Benetta, Mr. J. Dupond, Mr. P. Nappey and Mr. S. Reynaud from the CERN/EF division for the construction of the optical readout system. We are grateful to Mr. A. Braem from CERN for mirror evaporation and to Dr. J. Giomataris for the preparation of high purity TMAE.

This work was supported by the Kadoorie Family Endowment Fund - a project of the Fund for Higher Education and by the BSF US-Israel Research Grant No. 85-00280/1.

The localization resolution of a single light spot was measureed to be of σ=2.2 mm. With an average of 10 points per ring, the center – needed for particle tracking, or the radius – used for identification will be determined with a resolution of $\approx$1.1 mm or $\approx$0.8 mm, respectively. The detector resolution which is dominated by the electron diffusion in the conversion gap can be improved by raising the TMAE temperature (smaller conversion length) and raising the gas pressure. The chromatic aberration of the radiator can be reduced by using other gases in the radiator such as Freons[21].

The present optical readout system has certainly not been optimized for the final application to RICH. In the case of large area detectors, image intensifiers of larger diameters can be used in order to have a reasonable demagnification. If a larger gain is needed, another light amplification stage can be added. For most experiments the present CCD readout system has to be replaced by a faster one, in order to reduce dead-time. Several fast systems are presently being developed as, for example, the readout of scintillating fibers[22].

IEEE Trans. Nucl. Sci. **NS-28**, 478 (1981).

9. R.S. Gilmore, T.K. Gooch, W.L. Kwan, I.C. McArthur, J. Malos, J.P. Melot, R.J. Tapper and R.J. Wyley. Nucl. Instrum. Methods **206**, 189 (1983).
10. D.M. Potter. Nucl. Instrum. Methods **228**, 56 (1984).
11. T.K. Gooch, R.S. Gilmore, D.R.N. Jeffery, W.L. Kwan, T.J. Llewellyn, I.C. McArthur, J. Malos and R.J. Tapper. Nucl. Instrum. Methods **A241**, 363 (1985).
12. G. Charpak, Proc. Int. Symp. on Lepton and Photon Interactions at High Energies, Kyoto 1985 (Kyoto Univ., Kyoto, 1985) p.514.
13. M. Suzuki, P. Strock, F. Sauli and G. Charpak. Nucl. Instrum. Methods **A254**, 556 (1987).
14. G. Charpak, J.P. Fabre, F. Sauli, M. Suzuki and W. Dominik. Nucl. Instrum. Methods **A258**, 177 (1987).
15. D. Sauvage, A. Breskin and R. Chechik. On the light emission yield from electron avalanches in TEA and TMAE mixed with Argon-Hydrocarbons. In preparation.
16. M. Suzuki, A. Breskin, G. Charpak, E. Daubie, W. Dominik, J.P. Fabre, J. Gaudean, F. Sauli, D. Sauvage, P. Strock and T. Zeludziewicz. Preprint CERN-EP/86-137, Contribution to the 3rd meeting on advanced detectors, Pisa (1986).
17. Y. Nakato, M. Ozaki and H. Tsubomura. J. Phys. Chem. **76**, 2105 (1972).
18. R.A. Holroyd, J.M. Preses, C.L. Woody and R.A. Johnson. Measurement of the

References

1. A. Breskin and R. Chechik. Nucl. Instrum. Methods **A252** (1986) 488.
2. R. Chechik and A. Breskin. On the properties of low-pressure TMAE-filled multistep UV-photon detectors. Preprint WIS-87/19/March-PH. Nucl. Instrum. Methods. In press.
3. P. Glässel, H. Ries, H. Specht, A. Breskin, R. Chechik, Z. Fraenkel and I. Tserruya. The electron pair spectrometer for NA34/2. CERN/HELIOS Note No. 135/March 1986.
4. A. Drees, P. Fischer, P. Glässel, G. Lamade, H. Ries, E. Schmoetten, H.J. Specht, A. Breskin, R. Chechik, Z. Fraenkel and I. Tserruya. A ring-imaging Čerenkov Counter with low-pressure two-step UV- detector. Presented at the London conf. on position sensitive detectors, London Sept. 1987. Nucl. Instr. Methods. In press.
5. See for example H.J. Burckhart, J. Vavra, K. Zankel, U. Dusziak, D. Schaile, Q. Schaile, P. Igo-Kemenes, P. Lennert. Nucl. Instrum. Methods **A244**, 416 (1986).
6. See for example D.R. Nygren and J.N. Marx, Physics Today, **31**, 46 (1978).
7. G.B. Coutrakon, B. Biggs and S. Dhawan, IEEE Trans. Nucl. Sci. **NS-33**, 205 (1986).

   P. Fischer et al., Univ. of Heidelberg, in preparation.
8. O. Siegmund, P. Sanford, I. Mason, L. Culhane, S. Kellock and R. Cockshott.

Figure captions

Fig. 1: Schematic diagram of the UV photon detector.

Fig. 2: Light emission spectrum of TMAE, excited by avalanche electrons in a parallel plate avalanche detector, using Ar (98%)+CH_4 (2%)+TMAE (23°C) mixture.

Fig. 3: Number of photons emitted, over 4π, by one electron in the avalanche, as a function of gas pressure and TMAE concentration, in C_2H_6 (70%)+Ar (30%)+TMAE mixture.

Fig. 4: Schematic view of the optical readout system.

Fig. 5: Four consecutive computer digitized events obtained with 5 GeV/c electrons. The squares indicate a recognized light spot. The circles represent ring fits. The pictures demonstrate the excellent signal/noise ratio, and the absence of any background and photon feedback.

Fig. 6: Number of photons in the recognized light spots. The exponential distribution is typical to a single electron spectrum at low amplification.

Fig. 7: A distribution of distances of light spots from the ring's center.

Fig. 8: Distribution of the number of recognized light spots per ring.

Fig. 9: Typical transmission and absorption curves for C_2H_6 and CH_4 gas, CaF_2 and two quartz windows, and the quantum efficiency curve of TMAE.

quantum efficiency of TMAE and TEA from threshold to 120mm. Paper 6408 submitted to the XXIII Int. Conf. on High Energy Physics, Berkeley, July 1986.

19. A. Breskin, R. Chechik, D. Sauvage and W. Dominik. A 3-stage gated low-pressure UV-detector with optical readout. In preparation.

20. A. Breskin, G. Charpak, S. Majewski, G. Melchart, G. Peterson and F. Sauli. Nucl. Instrum. Methods **161**, 19 (1979).

21. T. Ypsilantis, private communication.

22. R.E. Ansorge et al., Performance of a scintillating fibre detector for the UA2 upgrade. Preprint CERN-EP/87-63. Contribution to the Int. Conf. on Advances in Exp. Meth. for Colliding Beam Phys., SLAC March 1987.

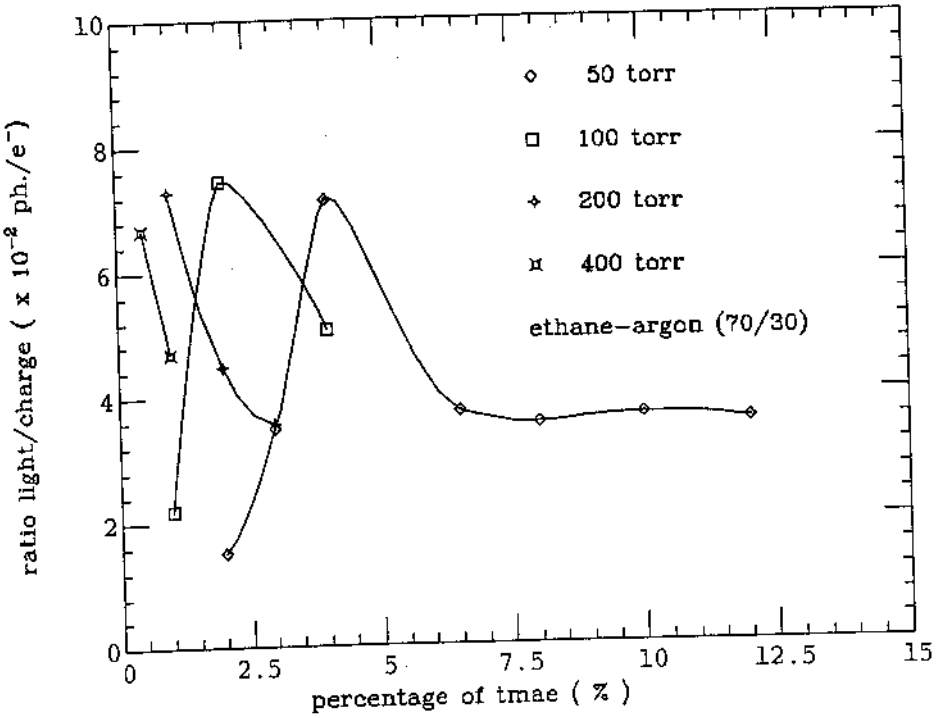
ratio light/charge (x 10^{-2} ph./e$^-$)
percentage of tmae (%)
50 torr
100 torr
200 torr
400 torr
ethane-argon (70/30)
0
2
4
6
8
10
0
2.5
5
7.5
10
12.5
15

Fig. 3

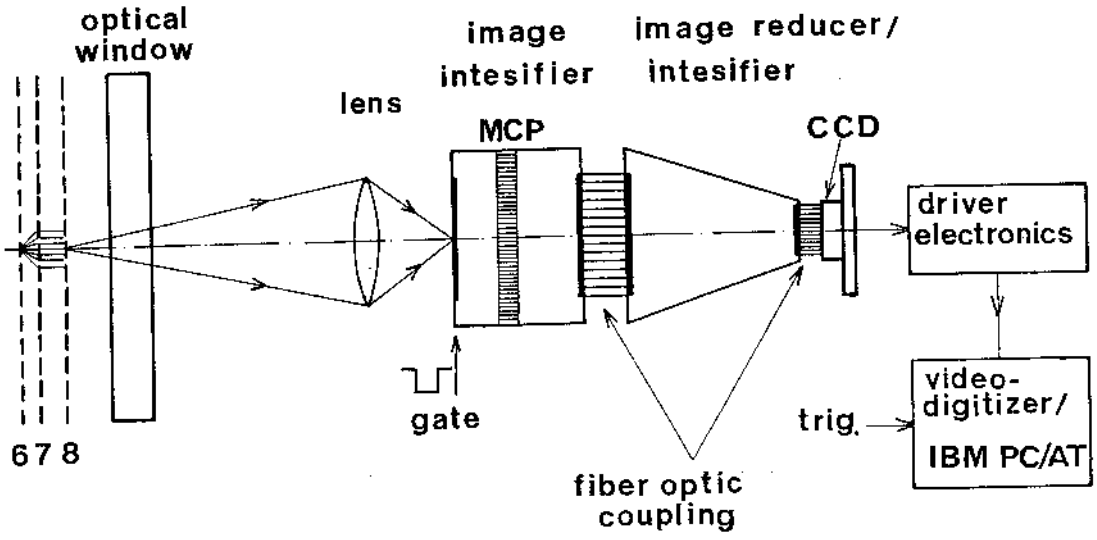
optical window
lens
image intesifier
MCP
image reducer/ intesifier
CCD
driver electronics
video-digitizer/ IBM PC/AT
trig.
gate
fiber optic coupling
6 7 8

Fig. 4

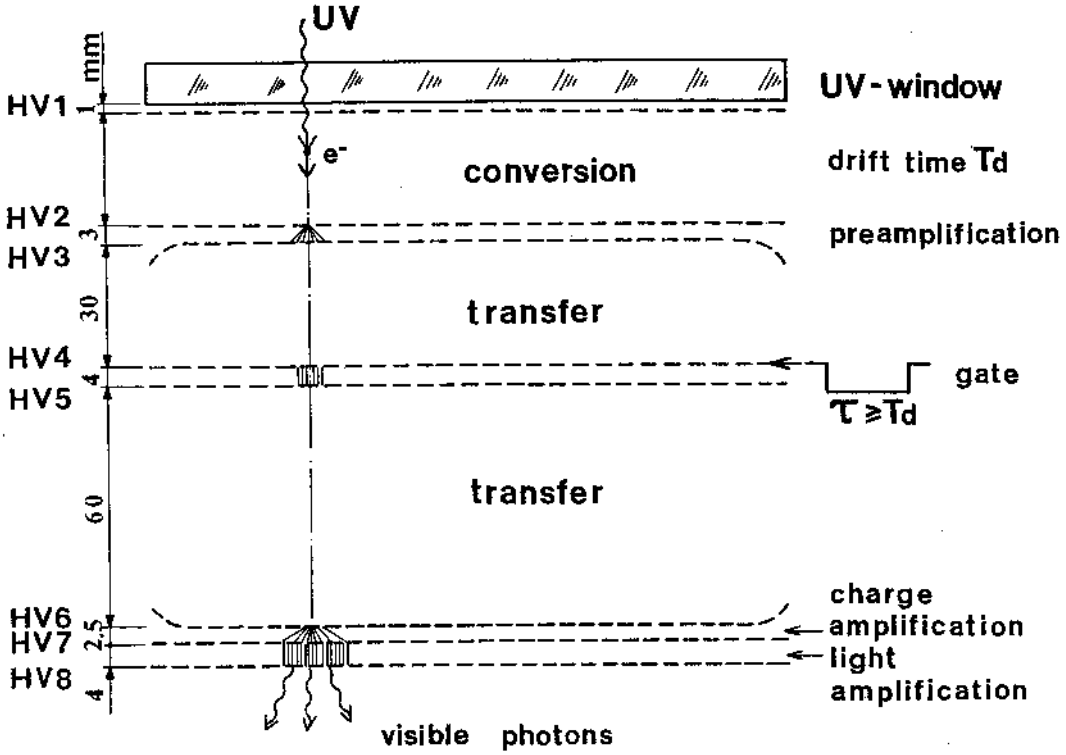
UV
mm
HV1
1
UV-window
e⁻
conversion
drift time Td
HV2
3
HV3
preamplification
30
transfer
HV4
4
HV5
gate
τ ≥ Td
60
transfer
charge
HV6
2.5
HV7
amplification
light
HV8
4
amplification
visible photons

Fig. 1

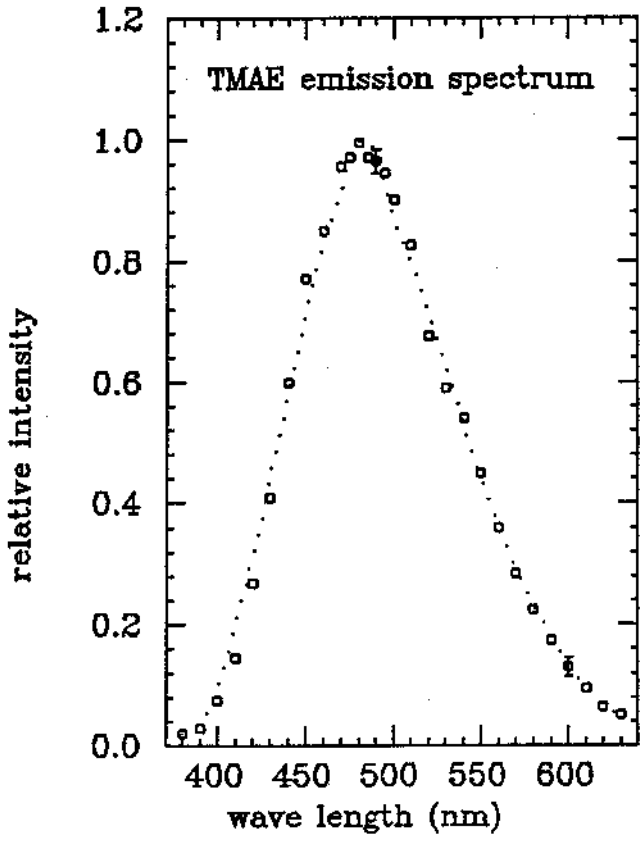
TMAE emission spectrum
relative intensity
1.2
1.0
0.8
0.6
0.4
0.2
0.0
400
450
500
550
600
wave length (nm)

Fig. 2

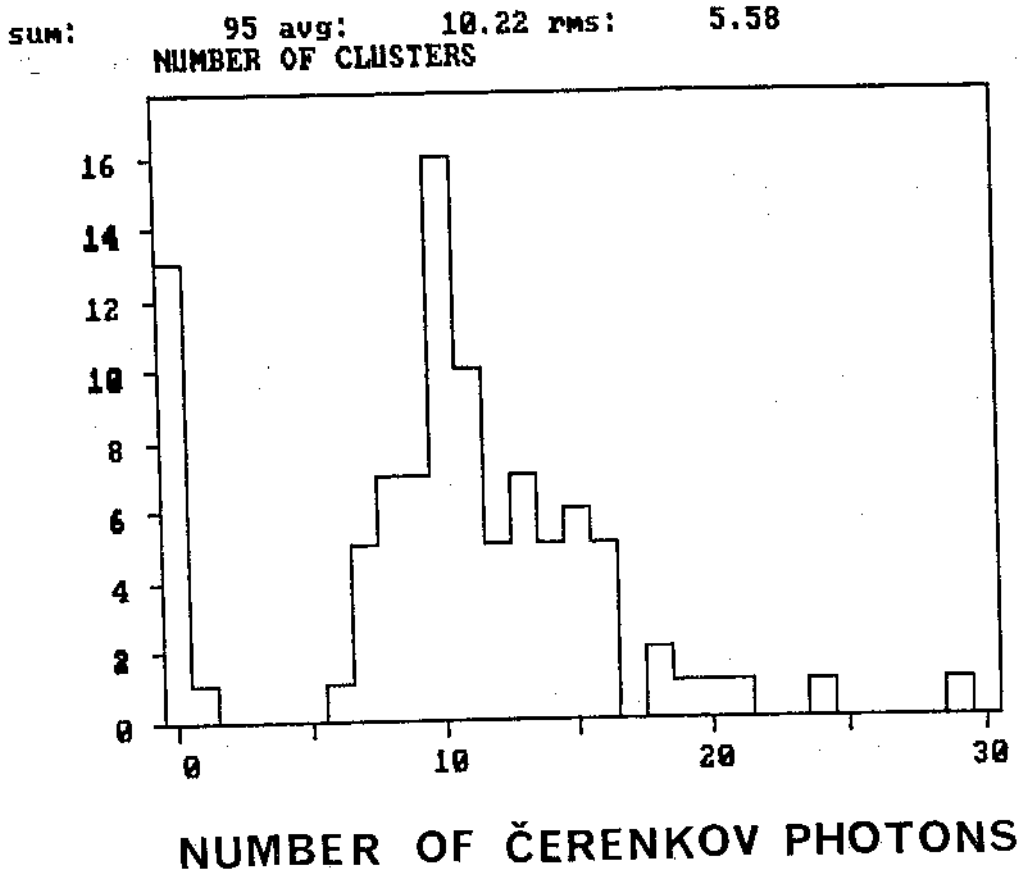
sum: 95 avg: 10.22 rms: 5.58
NUMBER OF CLUSTERS
16
14
12
10
8
6
4
2
0
0
10
20
30
NUMBER OF ČERENKOV PHOTONS

Fig. 8

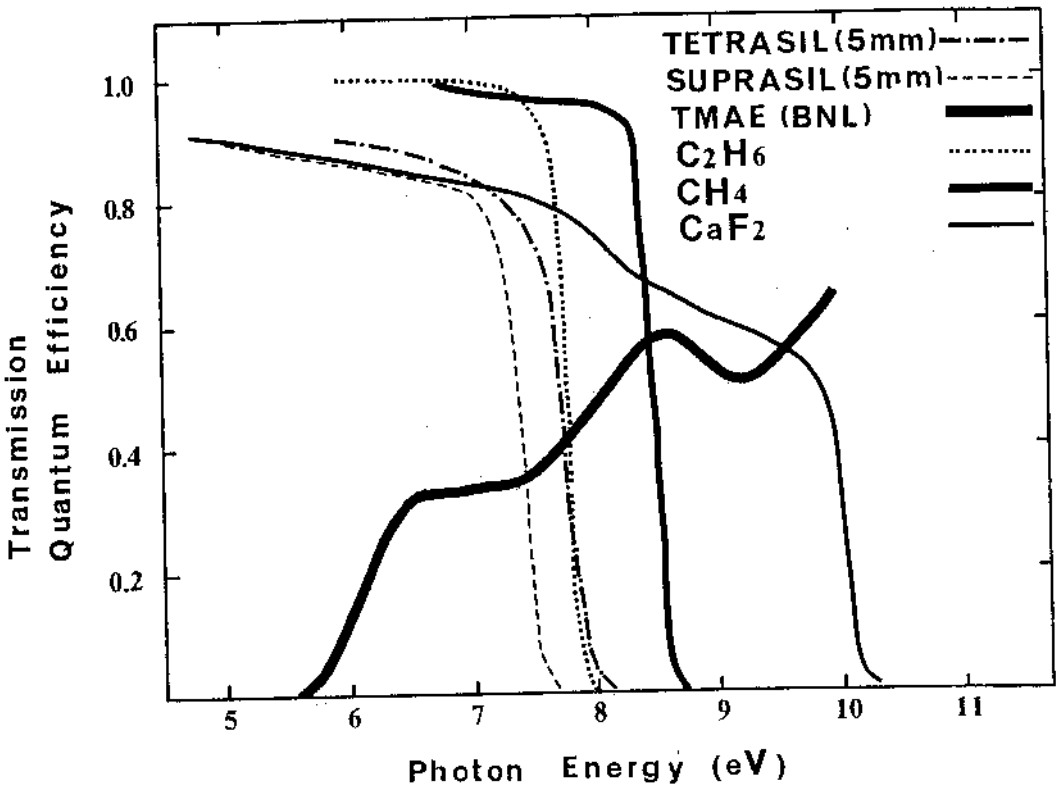
TETRASIL(5mm)
SUPRASIL(5mm)
TMAE (BNL)
C2H6
CH4
CaF2
Transmission
Quantum Efficiency
1.0
0.8
0.6
0.4
0.2
5
6
7
8
9
10
11
Photon Energy (eV)

Fig. 9

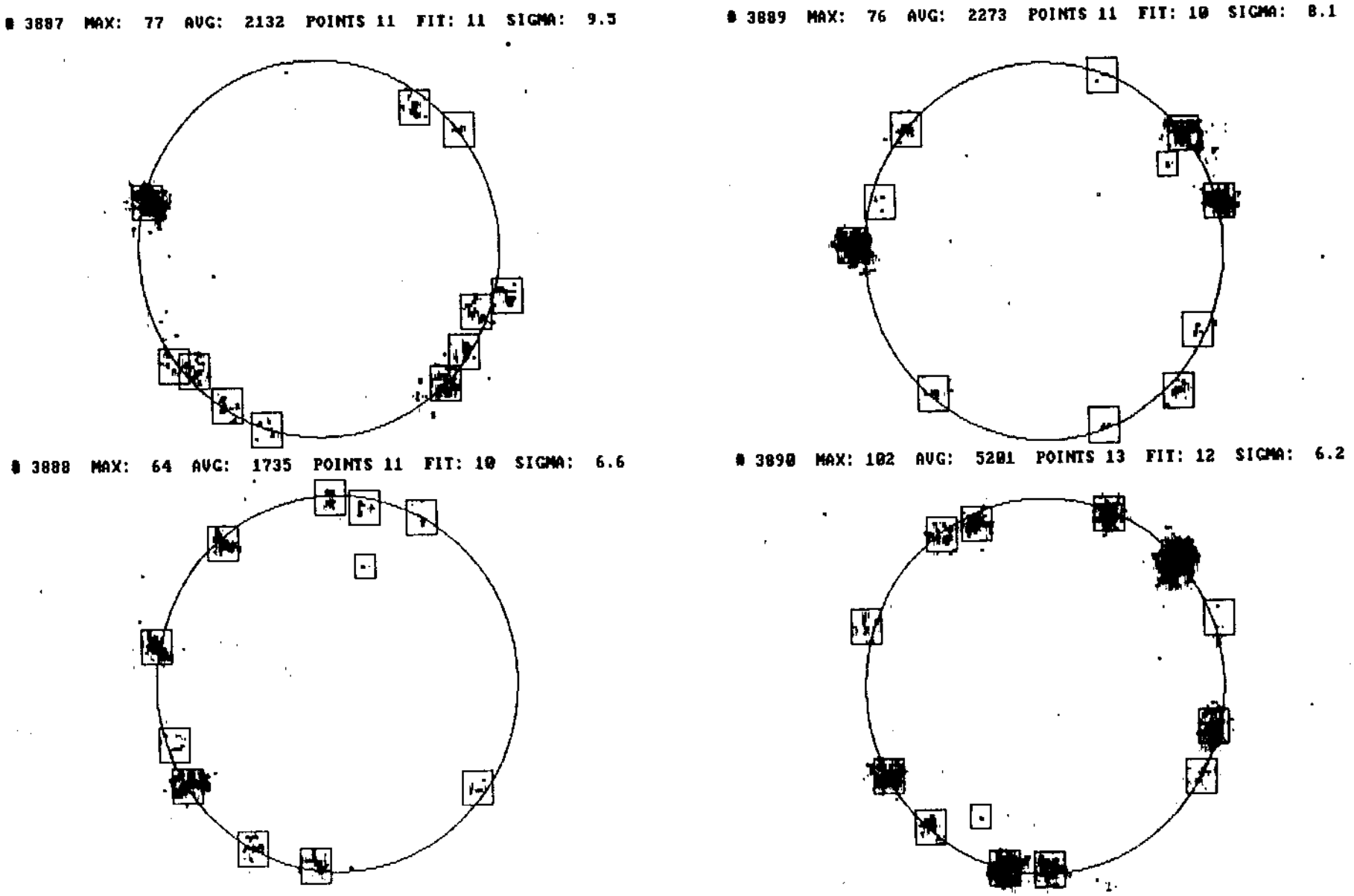
0 3887 MAX: 77 AVG: 2132 POINTS 11 FIT: 11 SIGMA: 9.5
0 3889 MAX: 76 AVG: 2273 POINTS 11 FIT: 10 SIGMA: 8.1
0 3888 MAX: 64 AVG: 1735 POINTS 11 FIT: 10 SIGMA: 6.6
0 3890 MAX: 102 AVG: 5201 POINTS 13 FIT: 12 SIGMA: 6.2

Fig. 5.

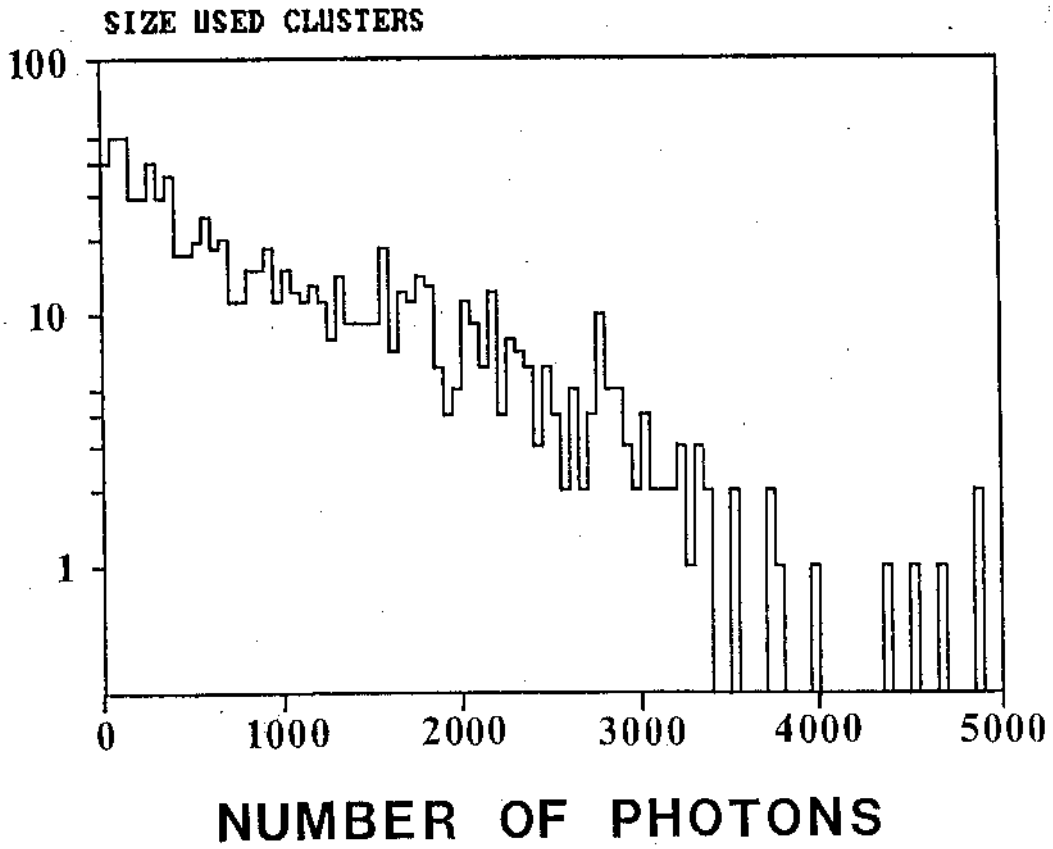
SIZE USED CLUSTERS
100
10
1
0
1000
2000
3000
4000
5000
NUMBER OF PHOTONS

Fig. 6

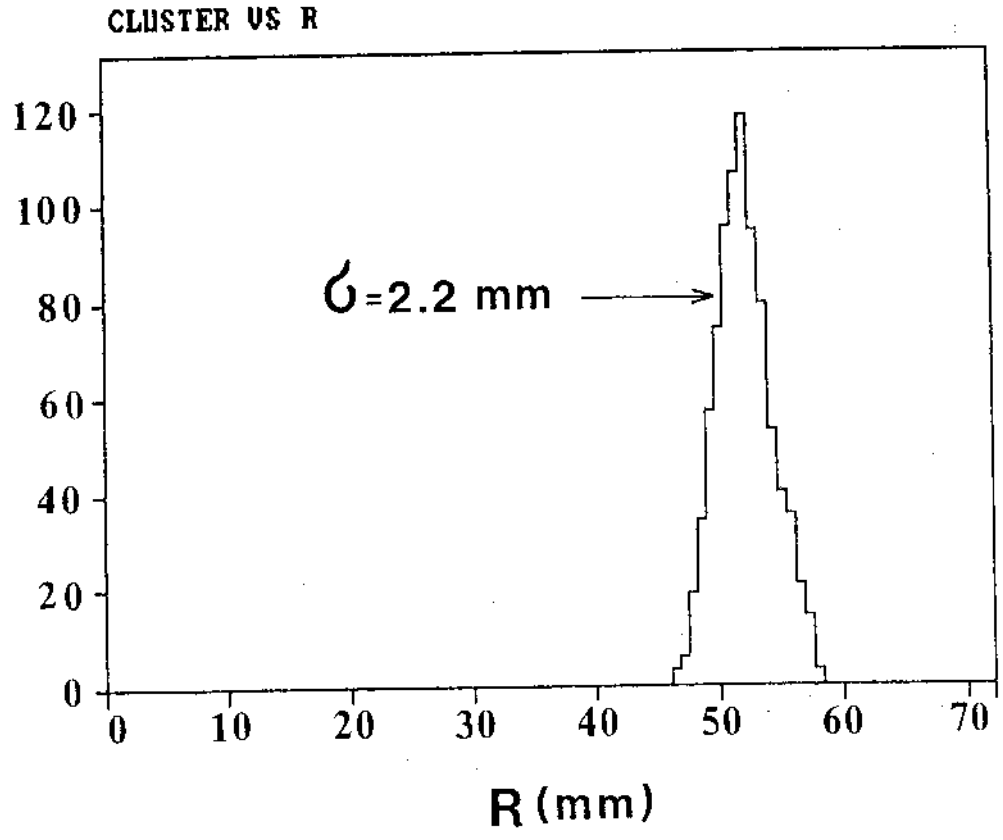
CLUSTER VS R
120
100
80
60
40
20
0
σ=2.2 mm
0
10
20
30
40
50
60
70
R (mm)

Fig. 7